Journal of Solid State Chemistry 182 (2009) 2274–2278

Contents lists available at ScienceDirect

Journal of Solid State Chemistry

journal homepage: www.elsevier.com/locate/jssc

Visible-light photocatalytic activity of the metastable $Bi_{20}TiO_{32}$ synthesized by a high-temperature quenching method

Hefeng Cheng [a], Baibiao Huang [a,*], Ying Dai [b], Xiaoyan Qin [a], Xiaoyang Zhang [a], Zeyan Wang [a], Minhua Jiang [a]

[a] State Key Lab of Crystal Materials, Shandong University, Jinan 250100, People's Republic of China
[b] School of Physics, Shandong University, Jinan 250100, People's Republic of China

ARTICLE INFO

Article history:
Received 13 March 2009
Received in revised form
29 May 2009
Accepted 6 June 2009
Available online 12 June 2009

Keywords:
Metastable phase
$Bi_{20}TiO_{32}$
Quenching
Photocatalytic activity

ABSTRACT

Metastable $Bi_{20}TiO_{32}$ samples were synthesized by a high-temperature quenching method using α-Bi_2O_3 and anatase TiO_2 as raw materials. The photocatalytic activity of the as-prepared samples was measured with the photodegradation of methyl orange at room temperature under visible light irradiation. The $Bi_{20}TiO_{32}$ samples exhibited good absorption in the visible light region with a band gap of about 2.38 eV and the band structure of $Bi_{20}TiO_{32}$ was studied. Photodegradation against methyl orange was much better than α-Bi_2O_3 prepared by the same way. The photocatalytic activity of $Bi_{20}TiO_{32}$ samples is supposed to be associated with the hybridized Bi 6*s* and O 2*p* orbitals. In addition, the dispersive characteristic of Bi 6*s* orbital in the hybridized valence band facilitates the mobility of the photogenerated carriers and hampers their recombination.

1. Introduction

In the past several decades, semiconductor photocatalysts have drawn much attention of the researchers for their application in environmental protection [1–4]. Undoubtedly, TiO_2 is the most extensively investigated material because it is nontoxic, easily available and stable to photocorrosion [2,5–7]. However, due to its large band gap (3.20 eV for anatase and 3.02 eV for rutile), TiO_2 is only responsive to ultraviolet irradiation which just accounts for a small proportion of the sunlight (about 4%). Moreover, the photoexcited electrons and holes easily tend to recombine, which results in the low quantum efficiency. Therefore, it is of great importance to exploit the novel photocatalyst systems, including modifications of TiO_2 [1,8,9], new visible-light compound photocatalysts [10–13] as well as semiconductor composites coupling [14,15]. Among them, the Bi-based oxides with an ns^2 configuration such as $BiVO_4$ [16–18], Bi_2WO_6 [19–21], $CaBi_2O_4$ [22], etc., catch the attention of the scientists due to the hybridized valence band (VB) by Bi 6*s* and O 2*p* orbitals that can be active under visible light irradiation. In addition, the activity of the materials is also influenced by the *s* composition in the valence band because the photoexcited carriers in *s* orbital have a high mobility due to its dispersive characteristic [23–25].

Bismuth titanates are of interest because they can be used as ferroelectric materials, actuators, capacitors, dielectric materials and photorefractive materials [26–29]. Bismuth titanates belong to a complicated system including several different phases such as $Bi_2Ti_2O_7$, $Bi_2Ti_4O_{11}$, $Bi_4Ti_3O_{12}$, $Bi_{12}TiO_{20}$, $Bi_{20}TiO_{32}$ and so forth. These phases are formed depending on the chemical compositions and processing conditions [30]. In earlier studies, Yao et al. found that pyrochlore $Bi_2Ti_2O_7$ [31], Aurivillius-type $Bi_4Ti_3O_{12}$ [32,33], sillenite $Bi_{12}TiO_{20}$ [34] show high photocatalytic activity for decomposing methyl orange. Among these bismuth titanates, $Bi_{12}TiO_{20}$ with a band gap of ca. 2.4 eV, displayed the highest photocatalytic activity which was considered to result from the Bi–O polyhedra of the $Bi_{12}TiO_{20}$ nanocrystals. Hou et al. reported that $Bi_{20}TiO_{32}$ nanocones were prepared by using a metal organic decomposition (MOD) method [35]. However, $Bi_{20}TiO_{32}$, metastable under ambient condition, existed merely as an impurity component during the formation of $Bi_2Ti_2O_7$ nanocrystals and transformed into $Bi_2Ti_2O_7$ phase thoroughly in 3 min at a temperature of 550 °C. According to the conventional phase diagram of Bi_2O_3–TiO_2 system, $Bi_{20}TiO_{32}$ phase is a metastable phase and could not emerge at a low temperature of 400 °C. The $Bi_{20}TiO_{32}$ phase cannot be fabricated by the traditional method in that when the molar ratio of Bi and Ti is over 10:1, the resulting product is not $Bi_{20}TiO_{32}$ but $Bi_{12}TiO_{20}$ [35,36]. With the mechanism of cooling from a relatively high temperature to a fairly low temperature in a very short period of time, quenching method is generally defined as "rapid cooling" of material [37]. Therefore, in comparison with the most of the traditional methods,

* Corresponding author. Fax: +86 531 8836 5969.
E-mail address: bbhuang@sdu.edu.cn (B. Huang).

0022-4596/$ - see front matter © 2009 Elsevier Inc. All rights reserved.
doi:10.1016/j.jssc.2009.06.006

quenching method is time-saving, low cost and rather simple. At the same time, the process of quenching or annealing has shown to lead to a variety of surface defects, strains, and reconstructions of materials which can optimize the performance of the material [38].

Herein, we fabricated the pure $Bi_{20}TiO_{32}$ metastable phase samples by a high-temperature quenching method and investigated its photocatalytic activity against methyl orange. To the best of our knowledge, it is the first time that the photocatalytic activity of this compound is getting reported. The band structure and the possible photocatalytic mechanism were also discussed.

2. Experimental details

2.1. Synthesis and characterization of the samples

$Bi_{20}TiO_{32}$ samples were prepared by a quenching method similar to Coskun et al.'s report [39]. TiO_2 (anatase) and α-Bi_2O_3 were both analytically pure grade and used without any purification. $Bi_{20}TiO_{32}$ was prepared by melting anatase TiO_2 and α-Bi_2O_3 (molar ratio 1:20) in a platinum crucible at 1000 °C for 2 min and subsequently quenched in water. Then the sample was ground in an agate mortar and the as-prepared sample was obtained. As a reference, α-Bi_2O_3 was treated by the same way. In addition, in order to study the influence of quenching process to the formation of $Bi_{20}TiO_{32}$ phase sample, the experiment was also carried out through natural cooling of the mixture of anatase TiO_2 and α-Bi_2O_3 (molar ratio 1:20) in furnace, after they were melted at 1000 °C for 2 min.

The as-prepared samples were characterized with X-ray powder diffraction (XRD, Bruker AXS D8 advance powder diffractometer with a Cu$K\alpha$ X-ray tube), to identify the crystal phases. The crystal morphology was characterized by scanning electron microscopy (SEM, Hitachi S-4800 microscope). UV–vis diffuse reflectance spectra were measured for the dry-pressed disk samples by a Shimadzu UV 2550 recording spectrophotometer equipped with an integrating sphere and $BaSO_4$ was used as a reference to measure all the samples. The spectra were recorded in the wavelength range 200–800 nm, allowing the study the optical absorption properties of the materials.

2.2. Photocatalytic reactions

The photocatalytic activity of the as-prepared samples was evaluated by degradation of methyl orange (MO) under visible light irradiation at room temperature. A 300 W Xe arc lamp (PLS-SXE300, Beijing Trusttech Co. Ltd.) equipped with an ultraviolet cutoff filter to provide visible light ($\lambda \geq 400$ nm) was used as the light source and the distance between the liquid surface of the suspension and the light source was about 10 cm. MO dye photodegradation was carried out with as-prepared powder (100 mg) suspended in MO aqueous solution (100 mL, 20 mg/L) in a 200 ml Pyrex glass vessel with constant stirring. Prior to the visible light irradiation, the suspensions were magnetically stirred in the dark for 50 min to establish adsorption/desorption equilibrium of MO dyes on the photocatalysts. At the given time intervals, about 5 ml of the suspension was taken from the reaction beaker for the analysis of MO concentration after centrifuging. The photocatalytic activities of the samples were evaluated by measuring the absorbance of aqueous methyl orange solution at 464 nm as a function of irradiation time with a UV–vis spectrophotometer (Shimadzu UV 2550).

3. Results and discussion

3.1. Crystal structure and morphology characterization

Fig. 1 shows the X-ray powder diffraction pattern of the as-prepared samples. We can clearly observe that all peaks of the sample quenched in water (Fig. 1b) are identical to the standard $Bi_{20}TiO_{32}$ phase (JCPDS 42-0202) and the sharp peaks indicate good crystallinity. The $Bi_{20}TiO_{32}$ phase belongs to the tetragonal system with the lattice constants $a = 7.700$ Å and $c = 5.653$ Å. The average grain size of the as-prepared sample is calculated to be about 53.9 nm with the (201) diffraction peak according to the Scherrer formula:

$$D = K\lambda(\beta \cos\theta)^{-1} \quad (1)$$

where D is the average grain diameter size of sample, λ is the wavelength of the X-ray radiation (i.e., $\lambda = 0.154056$ nm for Cu$K\alpha$ radiation), K is the Scherrer constant (K is usually determined about 0.9), θ is the X-ray diffraction angle, and β is the full width at half maximum (FWHM) of the (201) diffraction peak. In contrast, the sample which naturally cooled down in furnace (Fig. 1a) shows a mixed phase of $Bi_{12}TiO_{20}$ and α-Bi_2O_3, which were marked with maculae (•) and asterisks (*), respectively. It confirms that the $Bi_{20}TiO_{32}$ phase could not be prepared by the traditional methods but quenching method, and this may result from the reconstruction of material during the quenching process.

The SEM image of the as-prepared $Bi_{20}TiO_{32}$ sample is shown in Fig. 2. From the image above, we can see that the particle size of the sample is about 0.5–2 μm with an inhomogeneous particle size distribution. The particle size of the $Bi_{20}TiO_{32}$ samples from the SEM image is far bigger than the average grain size calculated according to the Scherrer formula and this may account for the particle agglomeration during the quenching process.

3.2. Optical absorption property and band structure calculation

Fig. 3A shows the UV–vis diffuse reflectance spectra of the samples. Both of the products exhibit good absorption in the visible region. The absorption edge of $Bi_{20}TiO_{32}$ locates approximately at 520 nm. For a crystalline semiconductor, the

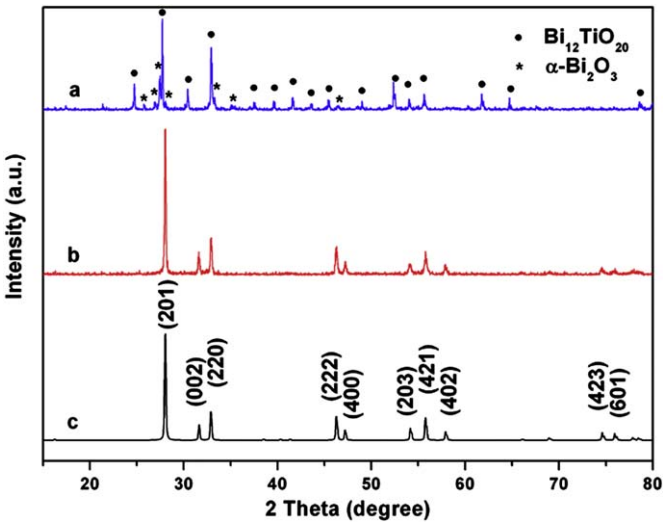

Fig. 1. XRD pattern of the as-prepared sample (a) naturally cooled down in furnace, (b) quenched in water, and (c) was the standard diffraction pattern for $Bi_{20}TiO_{32}$ taken from the JCPDS file (no. 42-0202).

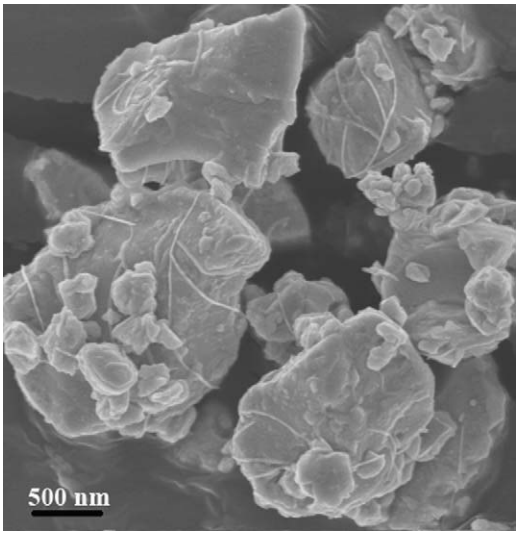

Fig. 2. SEM image of the as-prepared $Bi_{20}TiO_{32}$ sample.

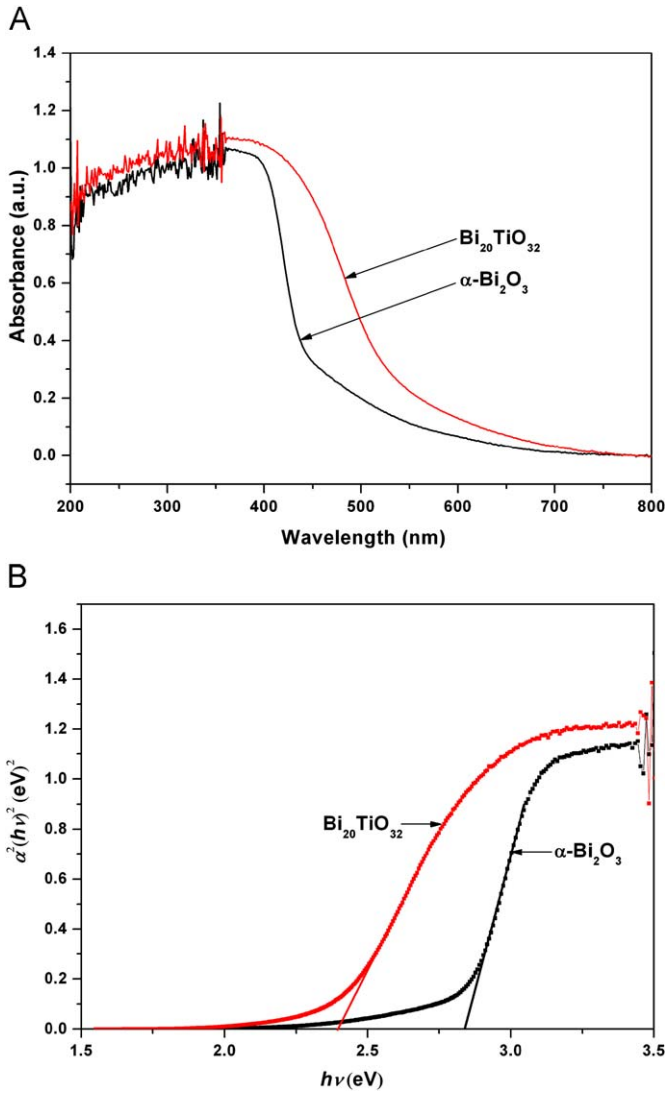

Fig. 3. (A) UV–vis diffuse reflectance spectra of the as-prepared $Bi_{20}TiO_{32}$ and α-Bi_2O_3 samples; (B) plots of $(\alpha h\nu)^2$ vs energy $(h\nu)$ for the band gap energies.

optical absorption near the band edge follows the equation [40,41]

$$\alpha h\nu = A(h\nu - E_g)^{n/2} \quad (2)$$

where α, ν, E_g, and A are absorption coefficient, light frequency, band gap, and a constant, respectively. According to the equation above, the value of n for $Bi_{20}TiO_{32}$ is 1. The band gap energy of the as-prepared $Bi_{20}TiO_{32}$ samples is determined from a plot of $(\alpha h\nu)^2$ vs energy $(h\nu)$ (Fig. 3B) and is found to be about 2.38 eV. In the same way, with the absorption spectra onset of about 440 nm, the band gap of α-Bi_2O_3 is found to be 2.82 eV. The colors of both oxides are consistent with their optical spectra; α-Bi_2O_3 is light yellow, while $Bi_{20}TiO_{32}$ is darker brownish yellow.

The band structure of the photocatalysts plays an important role in determining the photocatalytic property [41–43]. The conduction band (CB) and valence band potentials of the two semiconductors at the point of zero charge can be calculated by the following equation [44–47]:

$$E_{VB} = X - E^e + 0.5E_g \quad (3)$$

where E_{VB} is the VB edge potential, X is the absolute electronegativity of the semiconductor, expressed as the geometric mean of the absolute electronegativity of the constituent atoms which is defined as the arithmetic mean of the atomic electron affinity and the first ionization energy, E^e is the energy of free electrons on the hydrogen scale ($\approx$4.5 eV), and E_g is the band gap of the semiconductor. The CB edge potential could be determined by $E_{CB} = E_{VB} - E_g$. On the basis of the above equations, the top of the valence band and the bottom of the conduction band level of $Bi_{20}TiO_{32}$ are calculated to be +2.60 and +0.22 eV vs normal hydrogen electrode (NHE), respectively. The estimated band gap positions of anatase TiO_2, α-Bi_2O_3, and $Bi_{20}TiO_{32}$ are listed in Table 1.

The rough energy edge position of anatase TiO_2, α-Bi_2O_3, and $Bi_{20}TiO_{32}$ are shown in Fig. 4. In comparison with anatase TiO_2 and α-Bi_2O_3, the band gap of $Bi_{20}TiO_{32}$ is narrower, which means that $Bi_{20}TiO_{32}$ has better visible light absorption and can be excited more easily by irradiation to activate the photogenerated carriers.

3.3. *Visible-light photocatalytic activity of $Bi_{20}TiO_{32}$ samples*

The time-dependent UV–vis absorption spectra of MO dye during the irradiation is displayed in Fig. 5. It can be seen clearly that the maximum absorbance of 464 nm decreases greatly after irradiation in 180 min. Fig. 6 shows the photodegradation of MO dye as a function of irradiation time. The results show that after irradiation for 180 min, about 75.3% of MO dye molecules were degraded for $Bi_{20}TiO_{32}$ samples. In comparison, only 36.7% of MO dye molecules were degraded for α-Bi_2O_3 which was prepared by the same way in 180 min. In addition, the blank experiments were also carried out in the presence of $Bi_{20}TiO_{32}$ without irradiation or in the presence of irradiation without $Bi_{20}TiO_{32}$, from which we can observe that the MO dye cannot be degraded under visible light irradiation in the absence of photocatalysts.

In terms of practical use, the photocatalyst should be stable after several repeated experiments. As shown in Fig. 7, after five repeated cycles, the $Bi_{20}TiO_{32}$ can decompose the MO dye greatly except for a little decrease in photocatalytic activity, and this confirms that the as-prepared $Bi_{20}TiO_{32}$ samples was stable under irradiation for phototcatalytic decomposition of organic pollutants.

3.4. *Photocatalytic activity mechanism discussion*

In a typical photodegradation of organic pollutants process, when the semiconductor is irradiated by light, the photoexcited

Table 1
Electronegativity, estimated band gap, calculated energy edge position of valence and conduction band for antase TiO_2, α-Bi_2O_3, and $Bi_{20}TiO_{32}$.

Oxide semiconductors	Electronegativity (X)	Estimated E_g (eV)	Calculated VB position (eV)	Calculated CB position (eV)
Anatase TiO_2	5.810	3.2	2.91	−0.29
α-Bi_2O_3	5.919	2.82	2.83	0.01
$Bi_{20}TiO_{32}$	5.913	2.38	2.60	0.22

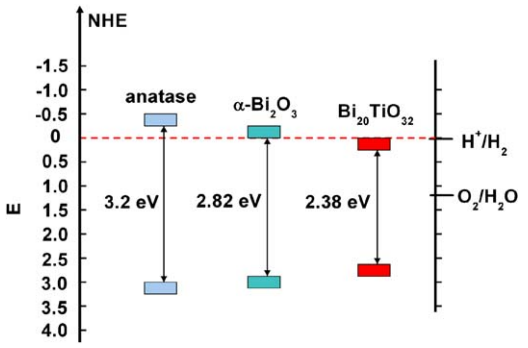

Fig. 4. The schematic diagram of the band structure of $Bi_{20}TiO_{32}$ samples.

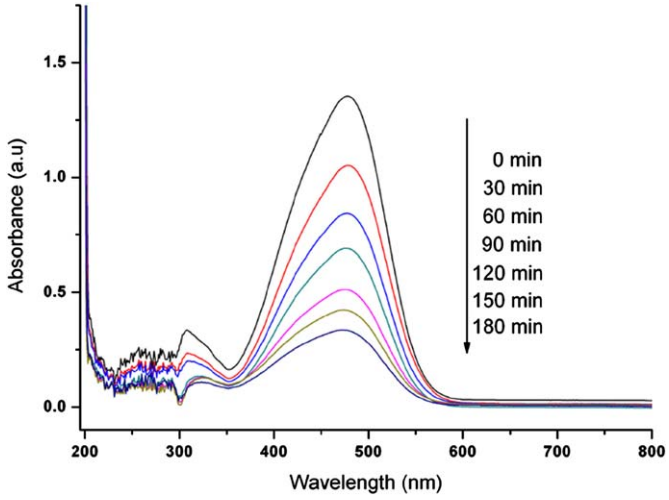

Fig. 5. The absorbance spectra changes of MO solution in the presence of $Bi_{20}TiO_{32}$ under visible light irradiation.

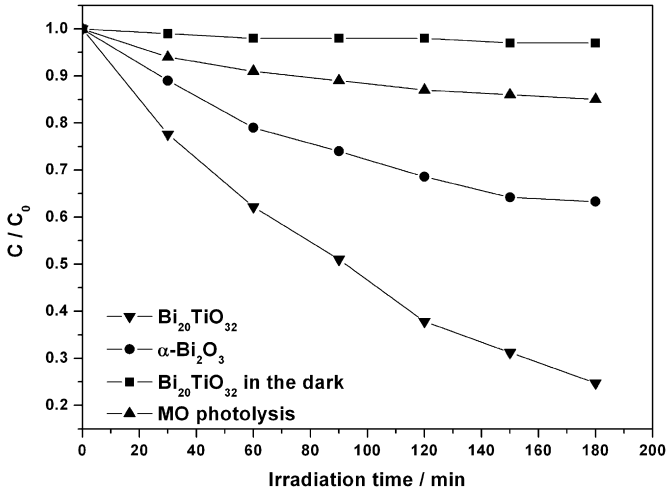

Fig. 6. The photodegradation of MO dye as a function of irradiation time.

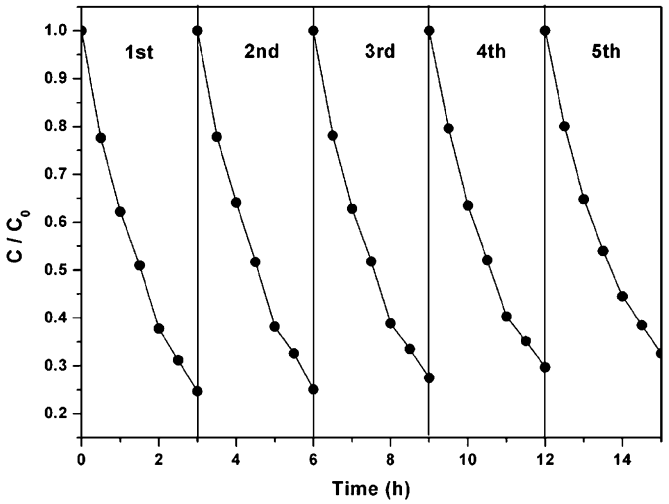

Fig. 7. Irradiation time dependence of photodegradation of MO dye over $Bi_{20}TiO_{32}$ during repeated experiment runs under visible irradiation.

electrons can be transferred to the conduction band from the valence band and whilst the holes form in the VB. Then the photoexcited holes in the VB or formed •OH oxidize the organic pollutants and the electrons in the CB participate in the oxidation process. So the photocatalytic activity of the semiconductor is very closely related to its corresponding band structure. The band gap of oxides is generally defined by the O 2*p* level and transition metal *d* level [34]. For the Bi-containing semiconductor with an ns^2 configuration, it was found that the valence band is hybridized by Bi 6*s* and O 2*p* orbitals. Based on the above consideration, we presume that the CB of $Bi_{20}TiO_{32}$ is composed of Ti 3*d* orbital and VB is composed of the hybridized Bi 6*s* and O 2*p* orbitals. The higher photocatalytic activity of $Bi_{20}TiO_{32}$ over α-Bi_2O_3 is considered to be in close relationship with the hybridized valence band, which meets the oxidation potential of the organic pollutants. Moreover, the large dispersity of VB which is induced by the hybridization of Bi 6*s* and O 2*p* orbitals facilitates the mobility of the photoexcited holes in VB [22].

4. Conclusions

Pure $Bi_{20}TiO_{32}$ metastable phase samples have been successfully synthesized by a high-temperature quenching method. The $Bi_{20}TiO_{32}$ samples exhibit good absorption in the visible light region with a band gap of about 2.38 eV and the photocatalytic activity against methyl orange is much better than α-Bi_2O_3 prepared by the same way. The photocatalytic activity of $Bi_{20}TiO_{32}$ samples is supposed to be associated with the hybridized Bi 6*s* and O 2*p* orbitals. In addition, the dispersive characteristic of Bi 6*s* orbital in the hybridized valence band facilitates the mobility of the photogenerated carriers and hampers their recombination. The quenching method illustrates a feasible way to fabricate the metastable phase compounds which could not be fabricated by the traditional method due to their instability under ambient

condition. At the same time, the metastable phase materials open up a new approach to the photocatalysts and will have promising potential application in photocatalysis.

Acknowledgments

This work was financially supported by a research Grant from the National Basic Research Program of China (no. 2007CB613302) and the National Natural Science Foundation of China (nos. 50721002 and 10774091).

References

[1] R. Asahi, T. Morikawa, T. Ohwaki, K. Aoki, Y. Taga, Science 293 (2001) 269–271.
[2] M.R. Hoffmann, S.T. Martin, W. Choi, D.W. Bahnemann, Chem. Rev. 95 (1995) 69–96.
[3] H. Lachheb, E. Puzenat, A. Houas, M. Ksibi, E. Elaloui, C. Guilard, J.M. Herrmann, Appl. Catal. B 39 (2002) 75–90.
[4] W.F. Yao, X.H. Xu, J.T. Zhou, X.N. Yang, S.X. Shang, H. Wang, B.B. Huang, J. Mol. Catal. A Chem. 212 (2004) 323–328.
[5] A.L. Linsebigler, G.Q. Lu, J.T. Yates, Chem. Rev. 95 (1995) 735–758.
[6] V. Keller, P. Bernhardt, F. Garin, J. Catal. 215 (2003) 129–138.
[7] J.C. Yu, L.Z. Zhang, Z. Zheng, J.C. Zhao, Chem. Mater. 15 (2003) 2280–2286.
[8] A.M. Yu, G.J. Wu, F.X. Zhang, Y.L. Yang, N.J. Guan, Catal. Lett. 129 (2009) 507–512.
[9] D.D. Zhang, R.L. Qiu, L. Song, B. Eric, Y.Q. Mo, X.F. Huang, J. Hazard. Mater. 163 (2009) 843–847.
[10] A. Ishikawa, T. Takata, J.N. Kondo, M. Hara, H. Kobayashi, K. Domen, J. Am. Chem. Soc. 124 (2002) 13547–13553.
[11] X.C. Wang, K. Maeda, A. Thomas, K. Takanabe, G. Xin, J.M. Carlsson, K. Domen, M. Antonietti, Nat. Mater. 8 (2009) 76–80.
[12] A. Kudo, I. Tsuji, H. Kato, Chem. Commun. 17 (2002) 1958–1959.
[13] J.G. Yu, X.X. Yu, B.B. Huang, X.Y. Zhang, Y. Dai, Cryst. Growth Des. 9 (2009) 1474–1480.
[14] P. Wang, B.B. Huang, X.Y. Qin, X.Y. Zhang, Y. Dai, J.Y. Wei, M.-H. Whangbo, Angew. Chem. Int. Ed. 47 (2008) 7931–7933.
[15] Z.Y. Wang, B.B. Huang, Y. Dai, X.Y. Qin, X.Y. Zhang, P. Wang, H.X. Liu, J.X. Yu, J. Phys. Chem. C 113 (2009) 4612–4617.
[16] A. Kudo, K. Omori, H. Kato, J. Am. Chem. Soc. 121 (1999) 11459–11467.
[17] S. Tokunaga, H. Kato, A. Kudo, Chem. Mater. 13 (2001) 4624–4628.
[18] J. Yu, A. Kudo, Adv. Funct. Mater. 16 (2006) 2163–2169.
[19] J. Wu, F. Duan, Y. Zheng, Y. Xie, J. Phys. Chem. C 111 (2007) 12866–12871.
[20] J.G. Yu, J.F. Xiong, B. Cheng, Y. Yu, J.B. Wang, J. Solid State Chem. 178 (2005) 1968–1972.
[21] S.S. Yao, J.Y. Wei, B.B. Huang, S.Y. Feng, X.Y. Zhang, X.Y. Qin, P. Wang, Z.Y. Wang, Q. Zhang, X.Y. Jing, J. Zhan, J. Solid State Chem. 182 (2009) 236–239.
[22] J.W. Tang, Z.G. Zou, J.H. Ye, Angew. Chem. Int. Ed. 43 (2004) 4463–4466.
[23] J.W. Tang, Z.G. Zou, J.H. Ye, J. Phys. Chem. C 111 (2007) 12779–12785.
[24] W. Wei, Y. Dai, B.B. Huang, J. Phys. Chem. C 113 (2009) 5658–5663.
[25] N. Lakshminarasimhan, Y. Park, W. Choi, Chem. Phys. Lett. 452 (2008) 264–268.
[26] S.E. Cummins, L.E. Cross, J. Appl. Phys. 39 (1968) 2268–2274.
[27] S.P. Yordanov, I. Ivanov, C.P. Carapanov, J. Phys. D Appl. Phys. 31 (1998) 800–806.
[28] M.P. Petrov, S.L. Sochava, S.I. Stepanov, Opt. Lett. 14 (1989) 284–286.
[29] X.N. Yang, B.B. Huang, H.B. Wang, S.X. Shang, W.F. Yao, J.Y. Wei, J. Cryst. Growth 270 (2004) 98–101.
[30] W.F. Su, Y.T. Lu, Mater. Chem. Phys. 80 (2003) 632–637.
[31] W.F. Yao, H. Wang, X.H. Xu, J.T. Zhou, X.N. Yang, Y. Zhang, S.X. Shang, Appl. Catal. A 259 (2004) 29–33.
[32] W.F. Yao, X.H. Xu, H. Wang, J.T. Zhou, X.N. Yang, Y. Zhang, S.X. Shang, B.B. Huang, Appl. Catal. B 52 (2004) 109–116.
[33] W.F. Yao, H. Wang, S.X. Shang, X.H. Xu, X.N. Yang, Y. Zhang, M. Wang, J. Mol. Catal. A Chem. 198 (2003) 343–348.
[34] W.F. Yao, H. Wang, X.H. Xu, X.F. Cheng, J. Huang, S.X. Shang, X.N. Yang, M. Wang, Appl. Catal. A 243 (2003) 185–190.
[35] Y. Hou, M. Wang, X.H. Xu, H. Wang, S.X. Shang, D. Wang, W.F. Yao, J. Cryst. Growth 240 (2002) 489–494.
[36] H. Wang, L.W. Fu, S.X. Shang, X.L. Wang, M.H. Jiang, J. Phys. D Appl. Phys. 27 (1994) 393–395.
[37] P. Supphasrirongjaroen, P. Praserthdam, J. Panpranot, D. Na-Ranong, O. Mekasuwandumrong, Chem. Eng. J. 138 (2008) 622–627.
[38] M.A. Henderson, Surf. Sci. 355 (1996) 151–166.
[39] A. Coskun, A. Ekicibil, B. Ozcelik, K. Kiymac, Chin. J. Phys. 43 (2005) 372–383.
[40] M.A. Butler, J. Appl. Phys. 48 (1977) 1914–1920.
[41] J. Zeng, H. Wang, Y.C. Zhang, M.K. Zhu, H. Yan, J. Phys. Chem. C 111 (2007) 11879–11887.
[42] D.E. Scaife, Sol. Energy 25 (1980) 41–54.
[43] P. Wang, B.B. Huang, X.Y. Zhang, X.Y. Qin, Y. Dai, H. Jin, J.Y. Wei, M.-H. Whangbo, Chem. Eur. J. 14 (2008) 10543–10546.
[44] Y.I. Kim, S.J. Atherton, E.S. Brigham, T.E. Mallouk, J. Phys. Chem. 97 (1993) 11802–11810.
[45] M.A. Butler, D.S. Ginley, J. Electrochem. Soc. 125 (1978) 228–232.
[46] Y. Xu, M.A.A. Schoonen, Am. Mineral. 85 (2000) 543–556.
[47] M.C. Long, W.M. Cai, J. Cai, B.X. Zhou, X.Y. Chai, Y.H. Wu, J. Phys. Chem. B 110 (2006) 20211–20216.